Available online at http://www.journalcra.com

International Journal of Current Research
Vol. 5, Issue, 02, pp. 162-171, February, 2013

INTERNATIONAL JOURNAL OF CURRENT RESEARCH

ISSN: 0975-833X

RESEARCH ARTICLE

Modeling and Simulation in Plane Geometry of Dirt Deposit in Heat Exchangers by Deposit of Ice in varying system

[1]Quenum C. Alphonse, [1]Kossou C. Toussaint, [1]Assoudo Abdoulaye, [1,*]Ahouannou Clément, [1]Sanya Emile A., [2]Mezrhab Ahmed, and [3]Feidt Michel

[1]Polytechnic School of Abomey-Calavi, Laboratory of Energetic and Mechanic Applied (LEMA), Cotonou/Benin, Box 01-2009. **Corresponding author:* ahouannou_clem@yahoo.fr
[2]Mohamed Premier University, Laboratory of Mechanics and Energetics - 60000 Oudja, Morocco
[3]Laboratory of Energetics and Theoretical Mechanic Applied (LEMTA)2 avenue de la Forêt de Haye, Nancy/France, Box 160-54504 Vandoeuvre Cedex

ARTICLE INFO

Article History:
Received 10th November, 2012
Received in revised form
25th December, 2012
Accepted 19th January, 2013
Published online 14th February, 2013

Key words:
Exchanger, Plates,
Dirt, Simulation,
Coefficient of overheating.

ABSTRACT

This article is devoted to modeling the mechanism of fouling in heat exchangers plates unsteady. The used simulation is based on the monitoring of the evolution of the ice at the changing phase (solidification) in water flowing in a rectangular section pipe, externally cooled. Cooling is done so that the heat exchange coefficient is uniform between coolant in a turbulent flow and the wall. The problem, numerically solved by finite difference method, provided results that allowed the exploration of the effects of the most relevant parameters such as the coefficient overheated liquid, Biotand Reynolds numbers, the axial position, the cooling mode and temperature, the evolution of the ice layer simulating the deposit of dirt.

INTRODUCTION

Widely used in various industrial sectors (chemical, food, petrochemical,etc.)., Heat exchangers during operation, end by losing the heat transfer efficiency, accompanied by an increase in pressure loss. These are two consequences attributable to fouling [1,3, 2]. The fouling, deposits on the heat exchange surface increases the thermal resistance to the transfer in time, due to several factors [3, 5, 2, 4]: scaling, corrosion, reactions between compounds in solution, the presence of macro and microorganisms, solids suspension or colloid, condensation of liquid particles or solidification in liquid phase. The importance of studies on fouling exchangers lies in the fact that this deposit produces exorbitant financial cost, due to the overhead caused by over-collateralization and especially downtime required for maintenance of the thermal units [3, 5, 8, 14, 2]. Modeling will predict the state ofclogging and to better sizing heat exchangers [7,9-14, 15,17, 20]. The deposition of substances is a function of time. It can therefore be modeled by performing a balance that involves the speed of growth of the deposit that characterizes its overcrowding and speed its elimination by retraining. The theory of germination [4] and its abundant use has a large step forward in the modeling of fouling [3, 5, 7, 8, 10, 13, 14, 6, 15,17, 20]. The literature shows, however, that both methods, thermal and hydrodynamic are conventionally used in the study of the mechanism of fouling. The first method uses measurement of global exchange coefficient over time to estimate the thickness of fouling deposition [1, 2]. The second links the overall resistance to flow, depending on the weight or thickness of fouling deposit, to the loss charge [13, 14]. The respective limits of previous approaches [15] led to the attempt of treating the problem by combining the two now taking into account both thermal and mechanical degradation, an approach known as entropy [2, 15, 17, 20].This article is devoted to the study by simulation, in plane geometry and in unsteady regime, the fouling of heat exchangers, followed by the growth of a layer of deposit ice.

2. EQUIPMENT AND METHODOLOGY

2.1. Simulating device

It was considered a line of flat rectangular section, ensuring the flow of water in which the phase change (solidification). It is cooled by a cooling fluid in turbulent flow, through the wall of a copper plate, so that the heat exchange coefficient between the fluid and the wall is uniform. The Figure 1 is a schematic representation of the problem where 0x is the pipe axis and 0ythe normal to 0x taken at half-height. Upstream of the pipe, the dynamic regime is supposedestablished and temperature profile is supposed to be uniform.

2.2. Methodology and solving the problem in plane geometry

We solve the heat equation in two-dimensional in each phase and then using the balance sheet and the condition at the interface, constants are determined finite volume or finite differences Methods are much more commonly used. We chose to resolve the problem by the method of finite differences on the one hand, and chose the formulation U-V-P other. This choice was guided by a quick calculation of the Peclet number, which

was very large (greater than 1000) for all simulations and allowed us to neglect the axial conduction in the energy equation for the liquid and solid phases [16, 18, 17]. Then, the ratio x/y_p is large enough in the solid region, so it was the approximation that $\frac{\partial^2 \theta_s}{\partial x^2} \ll 1$. Moreover, for all simulations, the Reynolds number of the working fluid is greater than 100, which authorizes the adoption of the Prandtl hypothesis. Given that the study applies to plate heat exchangers, it is convenient to adopt for the modeling, a two-dimensional Cartesian coordinate system (x, y) with x the axial coordinate and y is the normal coordinate. Thus, the following equations to be solved are expressed in dimensional quantities:

Local continuity equation :

$$\frac{\partial \rho}{\partial t} + \frac{\partial(\rho.u)}{\partial x} + \frac{\partial(\rho.v)}{\partial y} = 0 \quad (1)$$

Projection of movement equation along **0X** axis:

$$\rho\left(\frac{\partial u}{\partial t} + u\frac{\partial u}{\partial x} + v\frac{\partial u}{\partial y}\right) = -\frac{\partial p}{\partial x} + \mu\left(\frac{\partial^2 u}{\partial x^2} + \frac{\partial^2 u}{\partial y^2}\right) \quad (2)$$

Energy equation in the liquid:

$$\rho_l C_{pl}\left[\frac{\partial T_l}{\partial t} + u\frac{\partial T_l}{\partial x} + v\frac{\partial T_l}{\partial y}\right] = \lambda_l\left[\frac{\partial^2 T_l}{\partial x^2} + \frac{\partial^2 T_l}{\partial y^2}\right] + 2\mu\left[\left(\frac{\partial u}{\partial x}\right)^2 + \left(\frac{\partial v}{\partial y}\right)^2\right] + \mu\left[\frac{\partial v}{\partial x} + \frac{\partial u}{\partial y}\right]^2 \quad (3)$$

Energy equation in the solid:

$$\rho_s C_{ps}\frac{\partial T_s}{\partial t} = \lambda_s\left(\frac{\partial^2 T_s}{\partial x^2} + \frac{\partial^2 T_s}{\partial y^2}\right) \quad (4)$$

Where u and v denote the axial and normal speed components, S is the source term from the viscous dissipation of energy.
The main objective of the study was to determine the thickness of the deposit ice (fouling), we must add to these equations, the balance of the solid-liquid interface.

Energy equation in the solid-liquid interface:

$$\rho_s L\frac{\partial \delta}{\partial t} = \left[\lambda_s\frac{\partial T_s}{\partial y} - \lambda_l\frac{\partial T_l}{\partial y}\right]\left[1 + \left(\frac{\partial \delta}{\partial x}\right)^2\right] \quad (5)$$

The factor $\left[1 + \left(\frac{\partial \delta}{\partial x}\right)^2\right]$, introduced by the authors [3, 4], is the term that accounts for the curvature of the solid-liquid interface. It is important to recognize some simplifying assumptions that allow neglecting the effects of changes in certain variables. Thus, we took into account for the modeling, the following assumptions:

- The fluid is incompressible;
- The flow is laminar;
- The dynamic regime is established and the temperature in the entry of the cooled zone is uniform.
- Specific heat and thermal conductivity are considered constant.
- Natural convection is negligible.

Local continuity equation:

The fluid is incompressible, we have $\boldsymbol{div\vec{V} = 0}$and then:

$$\frac{\partial u}{\partial x} + \frac{\partial v}{\partial y} = 0 \quad (6)$$

Equation of motion along 0x:

$$\rho_l\left(\frac{\partial u}{\partial t} + u\frac{\partial u}{\partial x} + v\frac{\partial u}{\partial y}\right) = -\frac{\partial p}{\partial x} + \mu\frac{\partial^2 u}{\partial y^2} \quad (7)$$

Energy equation in the liquid:

$$\rho_l C_{pl}\left(\frac{\partial T_l}{\partial t} + u\frac{\partial T_l}{\partial x} + v\frac{\partial T_l}{\partial y}\right) = \lambda_l\left(\frac{\partial^2 T_l}{\partial y^2}\right) + \mu\left(\frac{\partial u}{\partial y}\right)^2 \quad (8)$$

Energy equation in the solid:

$$\rho_s C_{ps}\frac{\partial \mathrm{T_s}}{\partial t} = \lambda_s\frac{\partial^2 T_s}{\partial y^2} \quad (9)$$

Energy equation in the solid-liquid interface:

$$\rho_s L\frac{\partial \delta}{\partial t} = \left[\lambda_s\frac{\partial T_s}{\partial y} - \lambda_l\frac{\partial T_l}{\partial y}\right]\left[1 + \left(\frac{\partial \delta}{\partial x}\right)^2\right] \quad (10)$$

Equation of conservation of the flow:

$\int_0^{yp} u.l.dy = cte$ for the zone without deposit (11-1)

$\int_0^{\delta} u.l.dy = cte$ for the area with deposit (11-2)

The problem we are trying to solve is called "evolution."Thus we must add to these partial differential equations, boundary and initial conditions.

Boundary conditions:

At the entrance:

$T_l(y, x = 0, t) = T_e$ $\quad v(y, x = 0, t) = 0,$ $\quad u(y) = \frac{3}{2}u_d\left[1 - \left(\frac{y}{y_p}\right)^2\right]$

At the interface: $u(y = \delta, x, t) = v(y = \delta, x, t) = 0$
The assumption of local thermodynamic equilibrium can also write: $T_l(y = \delta, x, t) = T_s(y = \delta, x, t) = T_f$
To the wall: $u(y = y_p, x, t) = v(y = y_p, x, t) = 0$, for the area without ice

$\lambda_l\left[\frac{\partial T_l}{\partial y}(y = y_p, x, t)\right] = -h_\infty(T_p - T_\infty)$, for the ice-free area
$\lambda_s\left[\frac{\partial T_s}{\partial y}(y = y_p, x, t)\right] = -h_\infty(T_p - T_\infty)$, for the area with ice.
On the x-axis: $\frac{\partial u}{\partial y}(y = 0, x, t) = \frac{\partial T_l}{\partial y}(y = 0, x, t) = v(y = 0, x, t) = 0$

2.3. Landau Transformation

For the study area remains fixed in time and space, we applied the transformation of Landau [10] in the liquid and solid phases. It substitutes the normal variable η by two dimensionless variables $\bar{\eta}$and ξ define in each area for liquid and solid phases, the following amounts:

$\bar{\eta} = \frac{\eta}{\bar{\delta}} = \frac{y}{\delta}\xi = \frac{\eta - \bar{\delta}}{1 - \bar{\delta}}$ $0 \le \bar{\eta},\ \xi \le 1$

Thus, the field of solving the problem in the normal direction is bounded by 0 and 1. This condition facilitates the solution of the Stefan problem. Derived using the transfer, changes in variables related to η can be expressed as follows [20].
In the liquid phase, we can write:

$$\left(\frac{\partial}{\partial\eta}\right)_x = \frac{1}{\bar{\delta}}\left(\frac{\partial}{\partial\bar{\eta}}\right)\ ;\ \left(\frac{\partial^2}{\partial\eta^2}\right)_x = \frac{1}{\bar{\delta}^2}\left(\frac{\partial^2}{\partial\bar{\eta}^2}\right)\ ;\ \left(\frac{\partial}{\partial X}\right)_\eta = \left(\frac{\partial}{\partial X}\right)_{\bar{\eta}} - \frac{\bar{\eta}}{\bar{\delta}}\frac{d\bar{\delta}}{dX}\frac{\partial}{\partial\bar{\eta}}$$

$$\left(\frac{\partial^2}{\partial X^2}\right)_\eta = \left(\frac{\partial^2}{\partial X^2}\right)_{\bar{\eta}} - \frac{2\bar{\eta}}{\bar{\delta}}\frac{d\bar{\delta}}{dX}\frac{\partial^2}{\partial\bar{\eta}\partial X} + \left[\frac{2\bar{\eta}}{\bar{\delta}^2}\left(\frac{d\bar{\delta}}{dX}\right)^2 - \frac{\bar{\eta}}{\bar{\delta}}\frac{d^2\bar{\delta}}{dX^2}\right]\frac{\partial}{\partial\bar{\eta}} + \frac{\bar{\eta}^2}{\bar{\delta}^2}\left(\frac{d\bar{\delta}}{dX}\right)^2\frac{\partial^2}{\partial\bar{\eta}^2}$$

In the solid phase, we have:

$$\left(\frac{\partial}{\partial\eta}\right)_x = \frac{1}{1 - \bar{\delta}}\frac{\partial}{\partial\xi}\ ;\ \left(\frac{\partial^2}{\partial\eta^2}\right)_x = \frac{1}{(1 - \bar{\delta})^2}\frac{\partial^2}{\partial\xi^2}\ ;\ \left(\frac{\partial}{\partial X}\right)_\eta = \left(\frac{\partial}{\partial X}\right)_\xi + \frac{\xi - 1}{1 - \bar{\delta}}\frac{d\bar{\delta}}{dX}\frac{\partial}{\partial\xi}$$

$$\left(\frac{\partial^2}{\partial X^2}\right)_\eta = \left(\frac{\partial^2}{\partial X^2}\right)_\xi + \frac{2(\xi - 1)}{1 - \bar{\delta}}\frac{d\bar{\delta}}{dX}\frac{\partial^2}{\partial X\partial\xi} + \left[\frac{2(\xi - 1)}{(1 - \bar{\delta})^2}\left(\frac{d\bar{\delta}}{dX}\right)^2 + \frac{\xi - 1}{1 - \bar{\delta}}\frac{d^2\bar{\delta}}{dX^2}\right]\frac{\partial}{\partial\xi} + \left(\frac{\xi - 1}{1 - \bar{\delta}}\right)^2\left(\frac{d\bar{\delta}}{dX}\right)^2\frac{\partial^2}{\partial\xi^2}$$

Equations written in dimensionless form By making dimensionless these equations and configuring using Landau transformations, we obtain the system consisting of equations written below:

Local continuity equation:

$$\frac{\partial U}{\partial X} - \frac{\bar{\eta}}{\bar{\delta}}\frac{d\bar{\delta}}{dX}\frac{\partial U}{\partial\bar{\eta}} + \frac{1}{\bar{\delta}}\frac{\partial V}{\partial\bar{\eta}} = 0 \quad (12)$$

Equation of motion along 0x:

$$\frac{\partial U}{\partial\tau} + \left(V - U\bar{\eta}\frac{d\bar{\delta}}{dX}\right)\frac{1}{\bar{\delta}}\frac{\partial U}{\partial\bar{\eta}} + U\frac{\partial U}{\partial X} - \frac{2}{Re\bar{\delta}^2}\frac{\partial^2 U}{\partial\bar{\eta}^2} = -\frac{dP}{dX} \quad (13)$$

Energy equation in the liquid phase:

$$\frac{\partial\theta_l}{\partial\tau} + U\left[\frac{\partial\theta_l}{\partial X} - \frac{\bar{\eta}}{\bar{\delta}}\frac{d\bar{\delta}}{dX}\frac{\partial\theta_l}{\partial\bar{\eta}}\right] + \frac{V}{\bar{\delta}}\frac{\partial\theta_l}{\partial\bar{\eta}} = \frac{2}{Pe\bar{\delta}^2}\frac{\partial^2\theta_l}{\partial\bar{\eta}^2} + \frac{2Br}{Pe\bar{\delta}^2}\left(\frac{\partial U}{\partial\bar{\eta}}\right)^2 \quad (14)$$

Energy equation in the solid phase:

$$\frac{\partial\theta_s}{\partial\tau} = \frac{2.Bi_l.St_l}{Pe.Bi_sSt_s}\frac{1}{(1-\bar{\delta})^2}\frac{\partial^2\theta_s}{\partial\xi^2} \quad (15)$$

Energy equation in the solid-liquid interface:

$$(1-\bar{\delta})\bar{\delta}\frac{\partial\bar{\delta}}{\partial\tau} = \frac{2Bi_lSt_l}{Pe.Bi_s}\left[\delta\frac{\partial\theta_s}{\partial\xi} - (1-\bar{\delta})\frac{\lambda_l}{\lambda_s}\frac{\partial\theta_l}{\partial\bar{\eta}}\right]\left[1+\left(\frac{\partial\bar{\delta}}{\partial X}\right)^2\right] \quad (16)$$

Conservation of flow equation:

$$\int_0^{\bar{\eta}=1} Ud\bar{\eta} = 1 \text{ for } \quad X \le X_f \quad (17\text{-}1)$$

$$\int_0^{\bar{\eta}=1} Ud\bar{\eta} = \frac{1}{\delta}\text{for} X > X_f \quad (17\text{-}2)$$

It accesses the dimensionless numbers that are:

- $Re = \frac{\rho_l u_d D_h}{\mu}$, Reynolds number characterizing the flow regime.
- $Pr = \frac{\mu C_{pl}}{\lambda_l}$, Prandtl number, binding velocity and temperature.
- $Pe = Re.Pr = \frac{\rho_l C_{pl} u_d D_h}{\lambda_l}$, Peclet number, ratio of axial conduction convection.
- $Br = \frac{\mu u_d^2}{\lambda_l(T_e - T_f)}$, number of Brinckman, taking into account the effects of viscous dissipation.
- $St_{l,s} = \frac{C_{pl,s}(T_e - T_f)}{L}$, Stefan number for the liquid and solid phases, respectively.
- $Bi_{l,s} = \frac{h_\infty.y_p}{\lambda_{l,s}}$, Biot number for the liquid and solid phases, respectively.
- $D_h = 4y_p$, hydraulic diameter and y_p the channel half height.

The boundary conditions become:

At the entrance:

$\theta_l(\bar{\eta}, X=0, \tau) = \theta_e V(\bar{\eta}, X=0, \tau) = 0\, U(\bar{\eta}, X=0, \tau) = \frac{3}{2}(1-\bar{\eta}^2)$
At the interface: $U(\bar{\eta}=1, X, \tau) = V(\bar{\eta}=1, X, \tau) = 0 \qquad for X > X_f\ \theta_l(\bar{\eta}=1, X, \tau) = \theta_s(\xi=0, X, \tau) = \theta_f for X > X_f$
At a wall: $U(\bar{\eta}, =1, X, \tau) = V(\bar{\eta}=1, X, \tau) = 0$
$\frac{\partial\theta}{\partial\bar{\eta}}(\bar{\eta}=1, X, \tau) = -Bi_l\bar{\eta}(\theta_p - \theta_\infty) for X \le X_f$
$\frac{\partial\theta_s}{\partial\xi}(\xi=1, X, \tau) = -Bi_s(1-\delta)(\theta_p - \theta_\infty) \quad for X > X_f$
On the axis: $\frac{\partial U}{\partial\bar{\eta}}(\bar{\eta}=0, X, \tau) = \frac{\partial\theta}{\partial\bar{\eta}}(\bar{\eta}=0, X, \tau) = V(\bar{\eta}=0, X, \tau) = 0$

The first and second derivatives contained in the partial differential equations of (12) to (17-2) were then calculated by respectively:

$$\frac{\partial\phi(i,j)}{\partial\bar{\eta}} = \frac{\phi(i,j+1) - \phi(i,j-1)}{2\Delta\bar{\eta}} + O(\Delta\bar{\eta})^2 \quad \frac{\partial\phi(i,j)}{\partial X} = \frac{\phi(i,j) - \phi(i-1,j)}{\Delta X} + O(\Delta X)$$

$$\frac{\partial^2\phi(i,j)}{\partial\bar{\eta}^2} = \frac{\phi(i,j+1) - 2\phi(i,j) + \phi(i,j-1)}{(\Delta\bar{\eta})^2} + O(\Delta\bar{\eta})^2 \quad \frac{\partial\phi(i,j)}{\partial\tau} = \frac{\phi_{(i,j)}^{t+1} - \phi_{(i,j)}^{t}}{\Delta\tau}$$

Discretization of the equations
Equation-energy in the liquid phase:
Equation (14) is in the form (18) and discretized as that of (19):

$$a_{1(j)}\frac{\partial\theta_f}{\partial\tau} + a_2(j)\frac{\partial\theta_l}{\partial\bar{\eta}} + a_3(j)\frac{\partial^2\theta_l}{\partial\bar{\eta}^2} + a_4(j)\frac{\partial\theta_l}{\partial X} = S(j) \quad (18)$$

$$a_1(j)\frac{\left[\left(\theta_1^{t+1}(i,j) - \theta_1^{t}(i,j)\right)\right]}{\Delta\tau} + a_2(j)\left[\frac{\theta_1^{t+1}(i,j+1) - \theta_1^{t+1}(i,j-1)}{2\Delta\bar{\eta}}\right] + a_3(j)\left[\frac{\theta_l^{t+1}(i,j+1) - 2\theta_l^{t+1}(i,j) + \theta_l^{t+1}(i,j-1)}{(\Delta\bar{\eta})^2}\right] + a_4(j)\left[\frac{\theta_l^{t+1}(i,j) - \theta_l^{t+1}(i-1,j)}{\Delta X}\right] = S(j) \quad (19)$$

where: $a_1(j) = 1$; $a_2(j) = \frac{V^{t+1}(i-1,j)}{\bar{\delta}^{t+1}(i-1)} - U^{t+1}(i-1,j)\frac{\bar{\eta}}{\bar{\delta}^{t+1}(i-1)}\frac{d\bar{\delta}^{t+1}}{dX}(i-1)$;

$a_3(j) = -\frac{2}{Pe\left(\bar{\delta}^{t+1}(i-1)\right)^2}$; $a_4(j) = U^{t+1}(i-1,j)$

$$S(j) = \frac{2Br}{Pe\left(\bar{\delta}^{t+1}(i-1)\right)^2}\left[\frac{U^{t+1}(i-1,j) - U^{t+1}(i-1,j-1)}{2\Delta\bar{\eta}}\right]^2$$

Rearranging the terms of the discretized equation of energy in the liquid, in ascending order of the indices j, we can rewrite it as (20):

$$a(j).\theta_l^{t+1}(i,j-1)+b(j).\theta_l^{t+1}(i,j)+c(j).\theta_l^{t+1}(i,j+1)=d(j) \qquad (20)$$

where: $a(j)=\frac{-a_2(j)}{2\Delta\bar{\eta}}+\frac{a_3(j)}{(\Delta\bar{\eta})^2}$; $b(j)=\frac{a_1(j)}{\Delta\tau}-\frac{2a_3(j)}{(\Delta\bar{\eta})^2}+\frac{a_4(j)}{\Delta X}$; $c(j)=\frac{a_2(j)}{2\Delta\bar{\eta}}+\frac{a_3(j)}{(\Delta\bar{\eta})^2}$

$$d(j)=\frac{a_1(j)}{\Delta\tau}\theta_l^t(i,j)+\frac{a_4(j)}{\Delta X}\theta_l^{t+1}(i-1,j)+S(j)$$

Thus, the vectors a (j) b (j) c (j) and (j) involve only the parameters of section i-1 are known at time t +1.
Equation (20), put in the matrix form (20'), provides a tri –diagonal:

$$\begin{bmatrix} b_1 & c_1 & 0 & \cdots & 0 \\ a_2 & b_2 & c_2 & \ddots & \vdots \\ 0 & \ddots & \ddots & \ddots & \vdots \\ \vdots & \ddots & \ddots & \ddots & 0 \\ \vdots & \ddots & a_{n-1} & b_{n-1} & c_{n-1} \\ 0 & \cdots & \cdots & 0 a_n & b_n \end{bmatrix} \begin{bmatrix} \theta_l(i,1) \\ \vdots \\ \vdots \\ \theta_l(i,j) \\ \vdots \\ \vdots \\ \theta_l(i,nj) \end{bmatrix} = \begin{bmatrix} 0 \\ d(2) \\ \vdots \\ d(j) \\ \vdots \\ \vdots \\ d(nj) \end{bmatrix} \qquad (20')$$

The elements b_1, c_1, a_n, b_n of the tri-diagonal matrix are determined using boundary conditions on the axis and the wall. We used the Thomas algorithm for solving this system and thus obtained, the temperature profile in the liquid. The same procedure was adopted in the following on the matrix representation of the other equations. Different coefficients of the matrices were then determined from the boundary conditions on the system to which they belong.

Energy equation in solid phase

Equation (15) is of the form:

$$a_{1(j)}\frac{\partial\theta_s}{\partial\tau}+a_2(j)\frac{\partial^2\theta_s}{\partial\xi^2}=0; \quad a_1(j)=1, a_2(j)=\frac{-2Bi_l.St_l}{Pe.Bi_sSt_s\left(1-\bar{\delta}^{t+1}(i)\right)^2} \qquad (21)$$

Its discretization gave (22) rearranged as (23) or matrix form (23')

$$a_1(j)\left[\frac{\theta_s^{t+1}(i,j)-\theta_s^t(i,j)}{\Delta\tau}\right]+a_2(j)\left[\frac{\theta_s^{t+1}(i,j+1)-2\theta_s^{t+1}(i,j)+\theta_s^{t+1}(i,j-1)}{(\Delta\xi)^2}\right]=0 \qquad (22)$$

$$a(j)\theta_s^{t+1}(i,j-1)+b(j)\theta_s^{t+1}(i,j)+c(j)\theta_s^{t+1}(i,j+1)=d(j) \qquad (23)$$

$$\begin{bmatrix} b_1 & c_1 & 0 & \cdots & 0 \\ a_2 & b_2 & c_2 & \ddots & \vdots \\ 0 & \ddots & \ddots & \ddots & \vdots \\ \vdots & \ddots & \ddots & \ddots & 0 \\ \vdots & \ddots & a_{n-1} & b_{n-1} & c_{n-1} \\ 0 & \cdots & \cdots & 0 a_n & b_n \end{bmatrix} \begin{bmatrix} \theta_s(i,1) \\ \vdots \\ \vdots \\ \theta_s(i,j) \\ \vdots \\ \vdots \\ \theta_s(i,nj) \end{bmatrix} = \begin{bmatrix} 0 \\ d(2) \\ \vdots \\ d(j) \\ \vdots \\ \vdots \\ d(nj) \end{bmatrix} \qquad (23')$$

It was determined, by identification, the vectors a(j), b(j), c(j) and d(j) respectively in sub- diagonal, diagonal, super-diagonal elements, and the result of the matrix product.

$$a(j)=\frac{a_2(j)}{(\Delta\xi)^2}; \qquad b(j)=\frac{a_1(j)}{\Delta\tau}-\frac{2a_2(j)}{(\Delta\xi)^2}; \qquad c(j)=\frac{a_2(j)}{(\Delta\xi)^2}; \qquad d(j)=\frac{a_1(j)}{\Delta\tau}\theta_s^t(i,j)$$

Elements b_1, c_1, a_n, b_n and are determined using boundary conditions at the interface and to the wall. The resolution of the tri-diagonal system gives the temperature profile in the solid.

Motion equation

At this stage of calculation, the temperature profiles in the liquid and the solid are known in every section i. We could therefore calculate the axial velocity profile. Equation (13) is then discretized in the following manner:

$$a_1(j)\left[\frac{U^{t+1}(i,j)-U^t(i,j)}{\Delta\tau}\right]+a_2(j)\left[\frac{U^{t+1}(i,j+1)-U^{t+1}(i,j-1)}{2\Delta\bar{\eta}}\right]+a_3(j)\left[\frac{U^{t+1}(i,j+1)-2U^{t+1}(i,j)+U^{t+1}(i,j-1)}{(\Delta\bar{\eta})^2}\right]+$$

$$a_4(j)\left[\frac{U^{t+1}(i,j)-U^{t+1}(i-1,j}{\Delta X}\right]+\left[\frac{P^{t+1}(i)-P^{t+1}(i-1)}{\Delta X}\right]=0 \qquad (24)$$

where: $a_1(j)=1$; $a_2(j)=\frac{V^{t+1}(i-1,j)}{\bar{\delta}^{t+1}(i)}-\frac{U^{t+1}(i-1,j)\bar{\eta}(j)}{\bar{\delta}^{t+1}(i)}\frac{d\bar{\delta}^{t+1}(i)}{dX}$

$a_3(j) = -\frac{2}{Re\left(\bar{\delta}^{t+1}(i)\right)^2}$; $\quad a_4(j) = U^{t+1}(i-1,j)$

Equation (24) rewritten as (25), has matrix representation (25'):

$$a(j)U^{t+1}(i,j-1) + b(j)U^{t+1}(i,j) + c(j)U^{t+1}(i,j+1) + \frac{P^{t+1}(i)}{\Delta X} = d(j) \quad (25)$$

with: $a(j) = -\frac{a_2(j)}{2\Delta\bar{\eta}} + \frac{a_3(j)}{(\Delta\bar{\eta})^2}$; $\quad b(j) = \frac{a_1(j)}{\Delta\tau} - \frac{2a_3(j)}{(\Delta\bar{\eta})^2} + \frac{a_4(j)}{\Delta X}$; $c(j) = \frac{a_2(j)}{2\Delta\bar{\eta}} + \frac{a_3(j)}{(\Delta\bar{\eta})^2}$ $d(j) = \frac{a_1(j)U^t(i,j)}{\Delta\tau} + \frac{a_4(j)U^{t+1}(i-1,j)}{\Delta X} + \frac{P^{t+1}(i-1)}{\Delta X}$

$$\begin{bmatrix} b_1 & c_1 & 0 & \cdots & 0 & 0 \\ a_2 & b_2 & c_2 & \ddots & 1/\Delta X & \\ 0 & \ddots & \ddots & \ddots & & \\ & \ddots & \ddots & \ddots & & \\ & \ddots & \ddots & 0 & \vdots & \\ \ddots & \ddots & a_{n-1} & b_{n-1} & c_{n-1} & 1/\Delta X \\ 0 & \ddots & \ddots & 0 & a_n b_n & 0 \\ 1/2 & \cdots & \cdots & \cdots & 0 & 0 \end{bmatrix} \begin{bmatrix} U(i,1) \\ \vdots \\ \vdots \\ U(i,j) \\ \vdots \\ \vdots \\ U(i,nj) \\ P(i) \end{bmatrix} = \begin{bmatrix} 0 \\ d(2) \\ \vdots \\ d(j) \\ \vdots \\ \vdots \\ d(nj) \\ d(nj+1) \end{bmatrix} \quad (25')$$

Local Continuity Equation

This is the equation of local continuity (12) which was used to calculate the normal component of the velocity V. The term $\partial V/\partial\bar{\eta}$is discretized by an upwind scheme in $\bar{\eta}$direction:

$$\frac{U^{t+1}(i,j) - U^{t+1}(i-1,j)}{\Delta X} - \frac{\bar{\eta}}{\bar{\delta}^{t+1}(i)}\frac{d\bar{\delta}^{t+1}(i)}{dX}\left[\frac{U^{t+1}(i,j+1) - U^{t+1}(i,j-1)}{2\Delta\bar{\eta}}\right] + \frac{1}{\bar{\delta}^{t+1}(i)}\left[\frac{V^{t+1}(i,j) - V^{t+1}(i,j-1)}{\Delta\bar{\eta}}\right] \quad (26)$$

Taking into account the second member, it gave the equation (27) written in the form:

$$a(j)V^{t+1}(i,j-1) + b(j)V^{t+1}(i,j) + c(j)V^{t+1}(i,j+1) = d(j) \quad (27)$$

with : $a(j) = \frac{1}{\bar{\delta}^{t+1}(i)\Delta\bar{\eta}}$; $\quad b(j) = \frac{1}{\bar{\delta}^{t+1}(i)\Delta\bar{\eta}}$; $\quad c(j) = 0$

$$d(j) = \left[\frac{U^{t+1}(i,j) - U^{t+1}(i-1,j)}{\Delta X}\right] + \frac{\bar{\eta}}{\bar{\delta}^{t+1}(i)}\frac{d\bar{\delta}^{t+1}(i)}{dX}\left[\frac{U^{t+1}(i,j+1) - U^{t+1}(i,j-1)}{2\Delta\bar{\eta}}\right]$$

This is a diagonal matrix whose bi-matrix representation is (27'):

$$\begin{bmatrix} b_1 & 0 & 0 & \cdots & \cdots & 0 \\ & a_2 b_2 & \ddots & \ddots & \ddots & \\ & 0 & \ddots & \ddots & \ddots & \\ & & \ddots & \ddots & \ddots & \\ & & \ddots & \ddots & 0 & \\ & & \ddots & a_{n-1} b_{n-1} & 0 & \\ 0 & & \cdots & \cdots & a_n b_n & \end{bmatrix} \begin{bmatrix} V(i,1) \\ \vdots \\ \vdots \\ V(i,j) \\ \vdots \\ \vdots \\ V(i,nj) \end{bmatrix} = \begin{bmatrix} 0 \\ d(2) \\ \vdots \\ d(j) \\ \vdots \\ d(nj-1) \\ 0 \end{bmatrix} \quad (27')$$

Energy equationin solid - liquid interface

Equation (16) is discretized as (28) and ordered:

$$\left(1 - \bar{\delta}^{t+1}(i)\right)\bar{\delta}^{t+1}(i)\left(\frac{\bar{\delta}^{t+1}(i) - \bar{\delta}^{t}(i)}{\Delta\tau}\right) = \frac{2Bi_l St_l}{Pe.Bi_s}\left[\bar{\delta}^{t+1}(i)\frac{\partial\theta_s}{\partial\xi} - \left(1 - \bar{\delta}^{t+1}(i)\right)\frac{\lambda_l}{\lambda_s}\frac{\partial\theta_l}{\partial\bar{\eta}}\right]$$

$$\left[1 - \frac{\left(\bar{\delta}^{t+1}(i)\right)^2 - 2\bar{\delta}^{t+1}(i).\bar{\delta}^{t+1}(i-1) + \left(\bar{\delta}^{t+1}(i-1)\right)^2}{(\Delta X)^2}\right] \quad (28)$$

It is then put into the form (29) of a third degree polynomial into$\bar{\delta}^{t+1}(i)$:

$$A.\left(\bar{\delta}^{t+1}(i)\right)^3 + B.\left(\bar{\delta}^{t+1}(i)\right)^2 + C\left(\bar{\delta}^{t+1}(i)\right) + D = 0 \quad (29)$$

With: $A = -\frac{1}{\Delta\tau} - \frac{2}{(\Delta X)^2}\frac{Bi_l St_l}{Pe.Bi_s}\left[\frac{\partial\theta_s}{\partial\xi} + \frac{\lambda_l}{\lambda_s}\frac{\partial\theta_l}{\partial\bar{\eta}}\right]$

$$B = \frac{1}{\Delta\tau}\left(1 + \bar{\delta}^{t}(i)\right) + \frac{2}{(\Delta X)^2}\frac{Bi_l St_l}{PeBi_s}\left[2\bar{\delta}^{t+1}(i-1)\frac{\partial\theta_s}{\partial\xi} + \frac{\lambda_l}{\lambda_s}\frac{\partial\theta_l}{\partial\bar{\eta}}\left(1 + 2\bar{\delta}^{t+1}(i-1)\right)\right]$$

$$C = -\frac{\bar{\delta}^{t}(i)}{\Delta\tau} - \frac{2Bi_l St_l}{PeBi_s}.\left[\left(1 + \left(\frac{\bar{\delta}^{t+1}(i-1)}{\Delta X}\right)^2\right)\frac{\partial\theta_s}{\partial\xi} + \frac{\lambda_l}{\lambda_s}\left(1 + \frac{\left(2 + \bar{\delta}^{t+1}(i-1).\bar{\delta}^{t+1}(i-1)\right)}{(\Delta X)^2}\right)\frac{\partial\theta_l}{\partial\bar{\eta}}\right] \; D = \frac{2Bi_l St_l}{Pe.Bi_s}.\frac{\lambda_l}{\lambda_s}.\frac{\partial\theta_l}{\partial\bar{\eta}}\left[1 + \left(\frac{\bar{\delta}^{t+1}(i-1)}{\Delta X}\right)^2\right]$$

Calculating the thickness of the deposit The best approach is that calculating $\bar{\delta}_{sta} and \left(d\bar{\delta}/dX\right)_{sta}$ from the heat equation in the solid steady, then introduce them into the heat balance in the interface (equation 16) forcalculatingtransient$\theta_s and \bar{\delta}$byNewton-Raphsoniterative method. Calculating approximate values of $\theta_s et \bar{\delta}$was then continued until the beginning of the formation of the deposit remains constant.
The dimensionless energy equation in solid, in steady state, is:

$$\frac{\partial^2 \theta_s}{\partial \xi^2} = 0 \qquad (30)$$

The boundary conditions below are added to the equation (30) for its analytical resolution:
At the interface,

we get : $\theta_s(\xi = 0, X) = \theta_l(\bar{\eta} = 1, X) = \theta_f$; $\quad \frac{\partial \theta_l}{\partial \bar{\eta}} = (\bar{\eta} = 1, X) \frac{\lambda_s}{\lambda_l} \frac{\bar{\delta}_{sta}}{(1-\bar{\delta}_{sta})} \frac{\partial \theta_s}{\partial \xi} (\xi = 0, X)$

At the wall,

we have: $\frac{\partial \theta_s}{\partial \xi} = \left(1 - \bar{\delta}_{sta}\right) Bi_s (\theta_s(\xi = 1, X) - \theta_\infty)$

The result of the analytical solution is such that $\bar{\delta}_{sta} = \frac{1+Bi_s}{Bi_s\left(1+\frac{\lambda_s}{\lambda_l}\frac{\theta_\infty}{\frac{\partial \theta_l}{\partial \bar{\eta}}}\right)}$

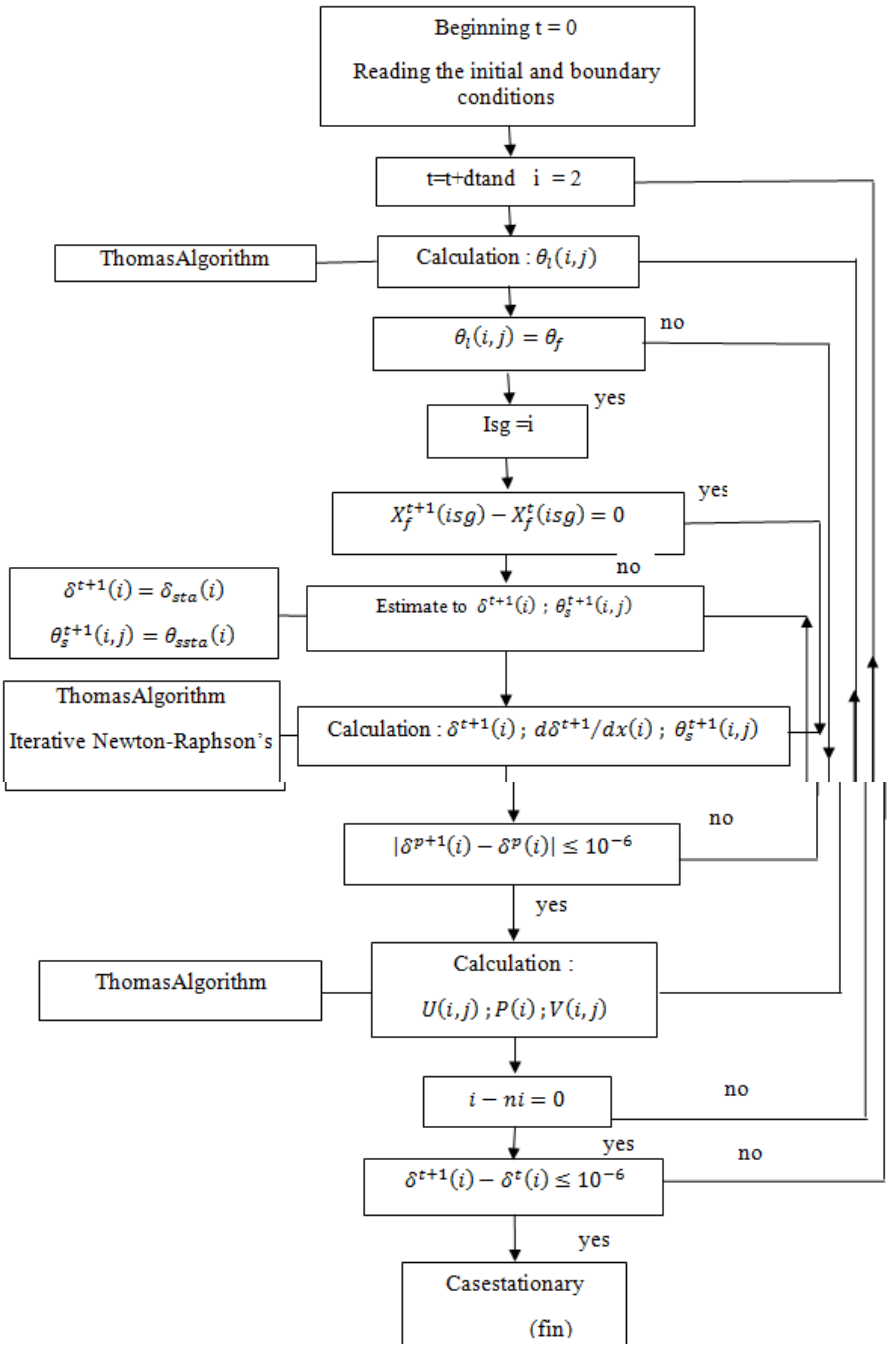

Figure 2. Flowchart of the algorithm for numerical computing in unsteady regime

There appears the expression of a gradient parietal whose values are very important for the calculation of the transfer of heat or pressure drop. Therefore, the choice of the polynomial approximation (29) must be judicious. The term commonly adopted is as follows:

$$\frac{\partial \phi}{\partial \bar{\eta}} = \frac{\phi(i,nj) - \phi(i,nj-1)}{\Delta \bar{\eta}} \qquad (31)$$

The results obtained with the expression (31) for calculating the temperature gradients at the wall and at the interface, are very strong. These are the source of a large velocity gradient. Itprefers for itself a third-degree polynomial, more accurate, given by (32):

$$\frac{\partial \phi}{\partial \bar{\eta}}(\bar{\eta} = 1, X, \tau) = c_0\phi(i,nj) + c_1\phi(i,nj-1) + c_2\phi(i,nj-2) + c_3(i,nj-3) \qquad (32)$$

where : $c_1 = 3$; $c_2 = -1/5$; $c_3 = 1/3$; $c_0 = -(c_1 + c_2 + c_3)$.

The flow chart describing the different steps of the algorithm calculations for the numerical solution is shown in Figure 2.

3. RESULTS AND DISCUSSION

Figure 3.1 (left) shows the results of analysis the overheating coefficient effects on the evolution of the solid - liquid interface relative to the selected position on the x axis. From these results, it is clear that when the coefficient overheating ε reduces, the appearance of ice deposit, so fouling occurs more rapidly, causing an enlargement of the area covered by fouling at the expense of naked without the ice. This has led to the search for limit position emergence of ice. It was then realized that the limit position is much smaller than the overheating coefficient is low still favoring development of the area covered.

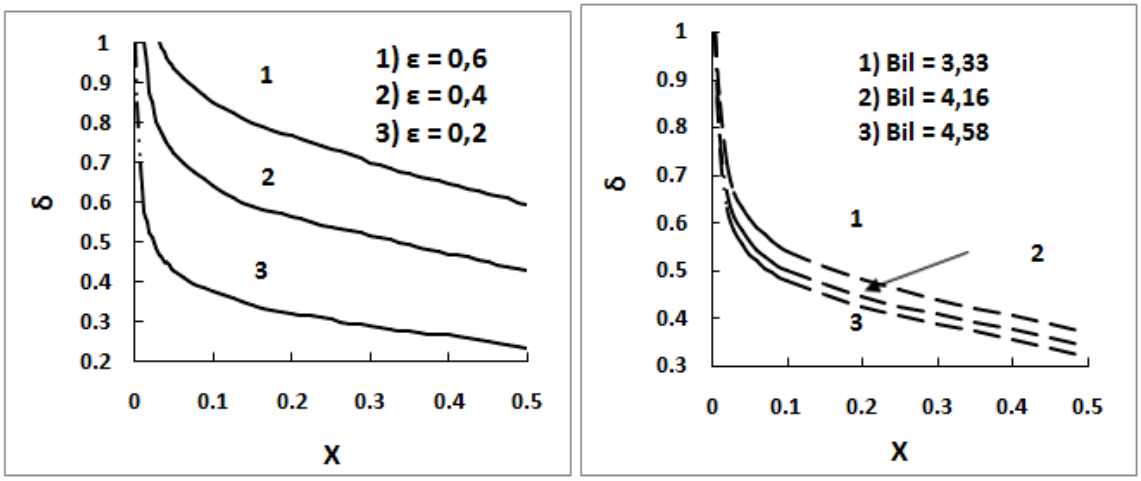

Figure 3.1 and 2. (3.1). Influences of overheating coefficienton the development of the solid-liquid interface as a function of the axial position, (3.2). with the liquid Biot number

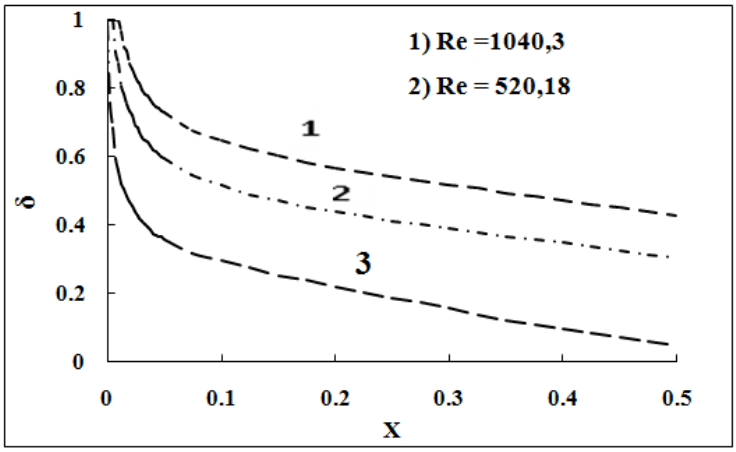

Figure 4. Effect of Reynolds number of the working fluid (for$\varepsilon = 0,4$ and $Bi_l = 1,66$)on the development of solid-liquid interface as a function of the axial position

The results presented in Figure 3.2 (right) are those arising from the influence of Biot number analysis on the evolution of deposit ice at fixed value of the overheating coefficient. It gets in effect increasing the liquid Biot number also causes enlargement of ice area at the expense of naked. Figure 4 presents results of analysis the effects of the Reynolds number or flow of the working fluid, on evolution of the ice according to the axial distance x. These results showed that the thickness of ice, simulating the thickness of dirt deposition, decreases as the Reynolds number or the flow rate increases at fixed Biot number and overheating coefficient values.

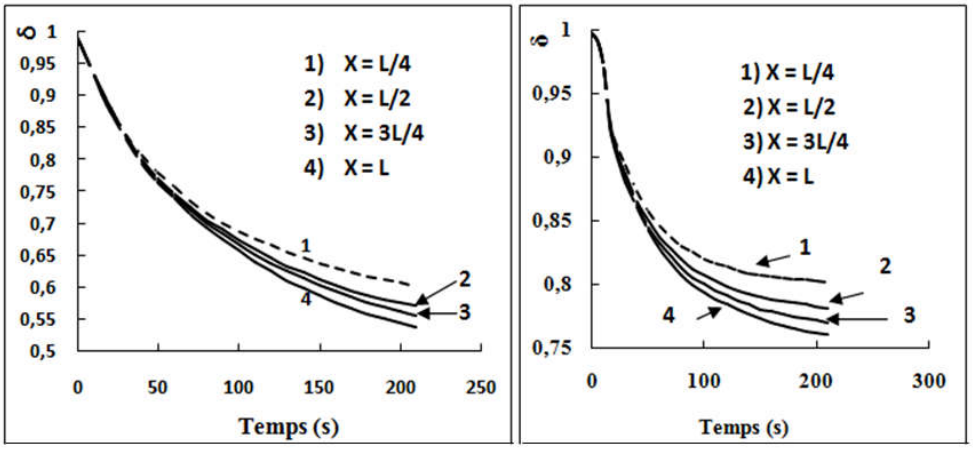

Figure 5. Effect of axial position on the evolution of the solid-liquid interface as a function of time (5.1-left): at $Bi_l = 4,58$; $Re = 520$; $\varepsilon = 0,2$, (5.1-left) and (5.2-right) : at$Bi_l = 4,58$; $Re = 520$; $\varepsilon = 0,3$

These Figures 5 show the results of the analysis ofice deposits profiles over time, in different sections (X) of the chilled water pipe (legends).The results given by these curves have led to conclusion that the deposition thickness increases as the water approaches the exit of the pipe. These results are entirely consistent, because this is a heat exchanger against the current in which the cooling water increases from the inlet to the outlet of the pipe, the area where its temperature significantly lower, promotes solidification. It should be noted that given section, the rate of growth of ice is relatively high in the first moments, but eventually experience slowdown at long times (time greater than 75 seconds). The results of the analysis of the effects of the axial position and the overheating coefficient in the temperature profile in the liquid and the plate are shown in Figure 6.

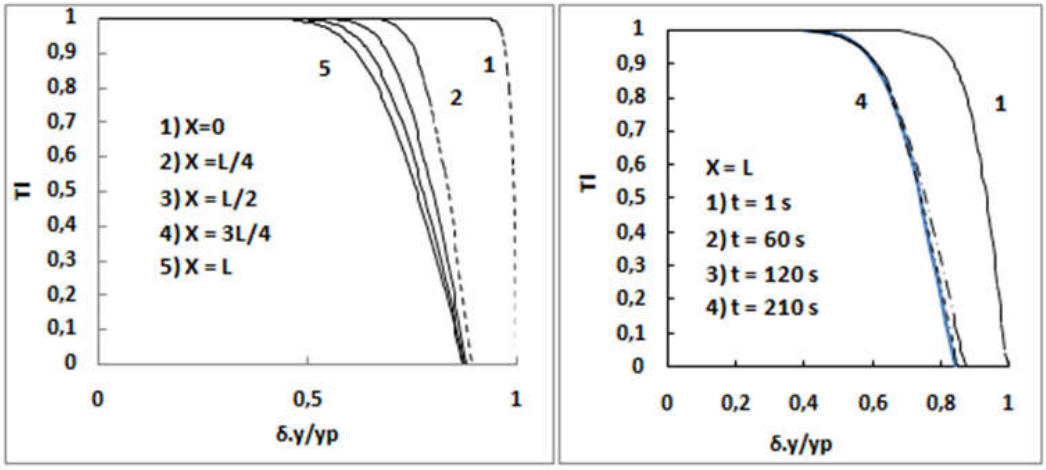

Figure 6. Influences of axial position and overheating coefficient on the temperature profile in liquid at the pipe outlet (asymmetrical cooling).

The results obtained here also are in no way inconsistent with those mentioned in various previous analyzes, as far as we are interested in those for temperature profiles based on both, the axial position, long times, the overheating coefficient, that the flow rate of the water. The examples shown in Figures 6 clearly show that the thermal boundary layer thickens up to the exit of the pipe area where the liquid is cold on one side and the temperature drop is higher in the first moments as long cooling time on the other. The curves obtained confirm that the higher the overheating coefficient is low, lower the temperature of plate. It is the same with the wall temperature when the Reynolds number of flowing water is low.

Conclusion

A model of plate heat exchanger fouling was described by the growth of ice based on a coupling of thermal degradation with the unsteady hydrodynamic. The simulation then allowed a better understanding of the influences of different parameters involved in the development and growth of the ice layer. It was thus possible to analyze the behavior of the thickness of the layer of ice (fouling deposit) as a function of the overheating coefficient, axial distance, and respective numbers of Biot liquid, Reynolds and finally time. Taking into account the experimental validation for the numerical model is the most perspective to this work.

REFERENCES

[1] Abu-Zaid M. (1992). A new technique for the measurement of fouling of heat transfer surfaces.Int. Comm. Heat Mass Transfer, Vol. 19, pp: 107-112.

[2] Anjorin M. (1993) Etude de l'encrassement d'échangeurs de chaleur. Nouvelles propositions sur les critères d'encrassement. Thèse de Doctorat Unique I.N.P. de Lorraine, décembre 208p.

[3] Bohnet M. *et al* (April, 1992). Fouling mechanisms.Theoretical and practical aspects. Seminar n°23 Proceedings Ed. EuropThet Ind. Grenoble,
[4] Clausse M. *et al* (1990). Germination phase.Entropy n° 153/154, pp: 33-39.
[5] Critteden B.D., Alderman N.J. (1992). Mechanisms by which fouling can increase overall heat transfer coefficients. Heattransfer engineering vol. 13 n°4, pp: 32-40
[6] Delaunay D. (1990). Transfert de chaleur par conduction associé à un changement de phase. 4e école d'été du G.U.T. Tome 1, Pont-à-Mousson, Juillet. pp: 327- 372.
[7] De Bonis M.V, RuoccoG (2009). Conjugate fluid flow and kinetics modeling for heat exchanger fouling simulation. *Internat. Journal of Thermal Sciences* 48, pp: 2006–2012.
[8] Knudsen J. (1981). Fouling of heat transfer surfaces: an overview in power condenser. Heat Transfer Technology, Marto, P. and Nunn, R. eds. Hemisphere Publishing corp. Washington, pp: 375-423.
[9] Lalof S,Palsson H. (2010).Detection of fouling in across-flow heat exchanger using a neuralnetwork based technique. *International Journal of Thermal Sciences*. Vol. 49, no4, pp: 675-679.
[10] Landau H. (1950). Heat conduction in a melting solid. Q. Appl. Math., Vol. 8, pp: 81- 94.
[11] Gut J.A.W, Pinto M. (2004). Modeling of plate heat exchanger with generalized configurations.*International Journal of Heat and Mass Transfer*, 46.pp : 2571-2585.
[12] Panya T., Phavanee N., Karn P. (2007). Dynamic Simulation of Plate and Frame Heat Exchanger Undergoing Rapid Fouling. *Proc. European Congress of Chem. Engineering (ECCE-6)* Copenhagen, 16-20 Sept. pp: 1-16.
[13] Ramasamy M., Shahid A., Zabiri H. (2008). Drift Analysis on Neural Network Model of Heat Exchanger Fouling. *Journal of Engineering Sci. and Technology*. Vol. 3(1), pp: 40-47.
[14] Radhakrishnan, V.R, Ramasamy, M., Zabiri, H., Do Thanh, V., Tahir, N.M, Mukhtar, H., Hamdi, M.R &Ramli, N. (2007). Heat exchanger fouling model and preventive maintenance scheduling tool. *Applied Thermal Engineering.*Vol.27, pp: 2791-2802.
[15] René F., Lalande M. (1987). Echangeur de chaleur à plaques et joints. Résolution numérique des équations d'échange thermique entre les différents canaux. Revue Générale de Thermique, n° 311. pp: 577-583.
[16] Sadeghipour M. S, Özisik M. N, Mulligan J. (1982). Transient Freezing of a liquid in a convectively cooled tube.Journal of Heat Transfer. Vol. 104, pp: 316-322.
[17] Sadouk H.C (2009). Modélisation de l'encrassement en régime turbulent dans un échangeur de chaleur à plaques avec un revêtement fibreux sur les parois. Thèse de Dctorat Unique, Université Paris-Est. 191p.
[18] Saito A., Okawa S., Kogabezawa S. (1991). Fundamental research on super cooling phenomenon on heat transfer surfaces: Investigation of freezing phenomenon of super cooled water droplet and its relationship with the effect of heat transfer surface. ASME/ J.S.M.E. Thermal Eng. Proc. Vol 3.pp: 319-326.
[19] Schreier P.J.R, Pritchard A.M., Fryer P.J. (1994). Heat exchanger fouling by whey protein solutions. Fouling and Cleaning Food Processing Congress, Cambridge, G.B.
[20] QuenumThe AC(1998).Study of fouling ofheat exchangersin plane geometrymodeling andexperimental simulationbyice.PhD thesisUniqueI.N.P.Lorraine, December.175p

****